Seismic response of three-dimensional rockfill dams using the Indirect Boundary Element Method

Article *in* IOP Conference Series Materials Science and Engineering · July 2010

DOI: 10.1088/1757-899X/10/1/012167

10 authors, including:

Juan Jose Perez-Gavilan E.
Universidad Nacional Autónoma de México
45 PUBLICATIONS **497** CITATIONS
SEE PROFILE

Martha Suarez
Universidad Nacional Autónoma de México
16 PUBLICATIONS **489** CITATIONS
SEE PROFILE

Humberto Marengo-Mogollon
Universidad Nacional Autónoma de México
31 PUBLICATIONS **92** CITATIONS
SEE PROFILE

Stéphanie Chaillat
French National Centre for Scientific Research
53 PUBLICATIONS **651** CITATIONS
SEE PROFILE

Seismic response of three-dimensional rockfill dams using the Indirect Boundary Element Method

2010 IOP Conf. Ser.: Mater. Sci. Eng. 10 012167

(http://iopscience.iop.org/1757-899X/10/1/012167)

Seismic response of three-dimensional rockfill dams using the Indirect Boundary Element Method

Francisco J. Sánchez-Sesma[1], Mauricio Arellano-Guzmán[1], Juan J. Pérez-Gavilán[1], Martha Suarez[1], Humberto Marengo-Mogollón[2], Stephanie Chaillat[3], Juan Diego Jaramillo[4], Juan Gómez[4], Ursula Iturrarán-Viveros[5] and Alejandro Rodríguez-Castellanos[6]

[1]*Universidad Nacional Autónoma de México; Instituto de Ingeniería, Cd. Universitaria, Circuito Escolar s/n; Coyoacán 04510; México D.F.; MEXICO*
[2] *Coordinación de Proyectos Hidroeléctricos, Comisión Federal de Electricidad, MEXICO*
[3] *Computational Science & Engineering, Georgia Institute of Technology, USA*
[4] *Departamento de Ingeniería Civil, Universidad EAFIT, Medellín, COLOMBIA*
[5] *Universidad Nacional Autónoma de México; Facultad de Ciencias, Cd Universitaria, Circuito Escolar s/n; Coyoacán 04510; México D.F.; MEXICO*
[6] *Instituto Mexicano del Petróleo, MEXICO*

E-mail: sesma@servidor.unam.mx

Abstract. The Indirect Boundary Element Method (IBEM) is used to compute the seismic response of a three-dimensional rockfill dam model. The IBEM is based on a *single layer* integral representation of elastic fields in terms of the full-space Green function, or fundamental solution of the equations of dynamic elasticity, and the associated force densities along the boundaries. The method has been applied to simulate the ground motion in several configurations of surface geology. Moreover, the IBEM has been used as benchmark to test other procedures. We compute the seismic response of a three-dimensional rockfill dam model placed within a canyon that constitutes an irregularity on the surface of an elastic half-space. The rockfill is also assumed elastic with hysteretic damping to account for energy dissipation. Various types of incident waves are considered to analyze the physical characteristics of the response: symmetries, amplifications, impulse response and the like. Computations are performed in the frequency domain and lead to time response using Fourier analysis. In the present implementation a symmetrical model is used to test symmetries. The boundaries of each region are discretized into boundary elements whose size depends on the shortest wavelength, typically, six boundary segments per wavelength. Usually, the seismic response of rockfill dams is simulated using either finite elements (FEM) or finite differences (FDM). In most applications, commercial tools that combine features of these methods are used to assess the seismic response of the system for a given motion at the base of model. However, in order to consider realistic excitation of seismic waves with different incidence angles and azimuth we explore the IBEM.

1. Introduction

Designing earth and rockfill dams in seismic zones require accounting to many factors that control the safety and usefulness of such complex systems. Simplified approaches have been developed that assume a shear beam model for the dam [1, 2] but capture significant aspects of 3D behavior and interaction with canyon.

Advanced three-dimensional (3D) boundary element methods (BEM) has been used for arch dams [3, 4] and the formulation includes a variety of effects: the water within the reservoir is assumed a compressible fluid, the dam and the foundation rock are assumed viscoelastic, and finally, the sediment is considered a poroelastic domain. Dynamic interaction among all those regions, local topography and travelling wave effects are taken into account as well. These developments for arch dams can be extended to earth and rockfill dams taking advantage of the experience gained studying the effects of surface geology on seismic ground motion.

In fact, surface geology may produce significant ground motion variations and may lead to large amplifications due to focusing and other phenomena. The physical basis of them are well understood (*e.g.* [5], [6], [7] and [8]); most of the uncertainty comes from incomplete knowledge of mechanical properties and geometry. Elastic inclusions like soft layering may induce resonances. These subjects may become of interest when dealing with the seismic response of earth and rockfill dams which share both irregular topography settings and sharp material contrasts. The advantage with respect to natural geological settings could be the more precise knowledge of the material and geometry.

In practice the seismic response of rockfill dams is simulated using either finite elements (FEM) or finite differences (FDM). It is frequent the use of commercial codes that combine features of these methods to assess the seismic response for a given motion at the base of model. However, in these methods it is difficult to consider the input of physically realistic seismic waves with different incidence angles and azimuth and the effects of nearby seismic sources as well.

For these reason, we explore the Indirect Boundary Element Method (IBEM) to study the seismic response of an idealized dam's model. At this stage, a very simple model with two planes of symmetry was selected for testing. We express scattered elastic waves using integral representations of the various elastic fields in terms of unknown force densities and the elastodynamic Green's function. The incoming seismic field is given by incidence of P, S and Rayleigh waves. This approach allows the specification of near source terms if required. Damping is usually introduced using an equivalent linear theory in which the quality factor $Q=1/2\xi$ with ξ=damping factor is a function of deformation and it is iteratively determined. In this work the quality factor is assumed constant. Frequency domain results and time histories at various curtain locations are analyzed.

2. The IBEM Method

The IBEM is used to solve the field equations of elasticity. It is based on a single layer integral representation of elastic fields in terms of the full-space Green function and force densities along the boundaries (e.g. [8] and [9]). The method has been applied with success to simulate the ground motion in several configurations of surface geology. Moreover, the IBEM has been used as reference to test other procedures.

Consider a domain V, bounded by surface S. If this domain is occupied by an elastic material, the diffracted displacement field under harmonic excitation can be written, neglecting body forces, by means of the single-layer boundary integral equation:

$$u_i(\boldsymbol{x}) = \int_S \phi_j(\boldsymbol{\xi}) G_{ij}(\boldsymbol{x};\boldsymbol{\xi}) dS_\xi, \tag{1}$$

where $u_i(\boldsymbol{x}) = i$th component of the displacement at point $\boldsymbol{x}$, $G_{ij}(\boldsymbol{x};\boldsymbol{\xi}) =$ Green's function, which is the displacement produced in the direction i at **x** due to the application of a unit force in direction j at point $\boldsymbol{\xi}$ within an infinite elastic space (we are using the frequency domain version of the Stokes' classical solution as given in [9]), $\phi_j(\boldsymbol{\xi}) =$force density in the direction j at point $\boldsymbol{\xi}$. The product $\phi_j(\boldsymbol{\xi})dS_\xi$ represents a distribution of forces at the surface S (the subscripts i,j are restricted to be 1, 2 or 3 and the summation convention is applied, *i. e.* a repeated subscript implies summation over its range, 1 to 3 in this case. Also u_1=u, u_2=v, and u_3=w). The subscript in the differential shows the variable over which the integration is carried out. This integral representation can be obtained from Somigliana's identity [8]. Moreover, it was proved that if $\phi_j(\boldsymbol{\xi})$ is continuous along S, then the displacements field is continuous across S [10].

This integral representation allows the calculation of stresses and tractions by means of the direct application of Hooke's law and Cauchy's equation, respectively, except at boundary singularities, that is, when $\boldsymbol{x}$ is equal to $\boldsymbol{\xi}$ on surface S. From a limiting process based on equilibrium considerations around an internal neighborhood of the boundary, it is possible to write, for $\boldsymbol{x}$ on S,

$$t_i(x) = c\phi_i(\boldsymbol{x}) + \int_S \phi_j(\boldsymbol{\xi})T_{ij}(\boldsymbol{x};\boldsymbol{\xi})dS_\xi, \tag{2}$$

where $t_i(\boldsymbol{x})$ is the ith component of traction, $c = 0.5$ if $\boldsymbol{x}$ tends to the boundary S from "inside" the region, $c = -0.5$ if $\boldsymbol{x}$ tends to S from "outside" the region, or $c = 0$ if $\boldsymbol{x}$ is not at S. $T_{ij}(\boldsymbol{x};\boldsymbol{\xi})$ is the traction Green's function, that is to say, the traction in the direction i at a point $\boldsymbol{x}$, associated to the unit vector $n_i(\boldsymbol{x})$, due to the application of a unit force in the direction j at $\boldsymbol{\xi}$ on S.

Eq.(1) and eq.(2) can be applied for 2D and 3D problems. The respective values of 2D and 3D Green functions for tractions and displacements can be consulted in [8] and [9], respectively.

3. Formulation of the problem

Starting from the configuration shown in Fig. 1, it is convenient to divide the domain in two regions (R and E), where adequate boundary conditions have to be established.

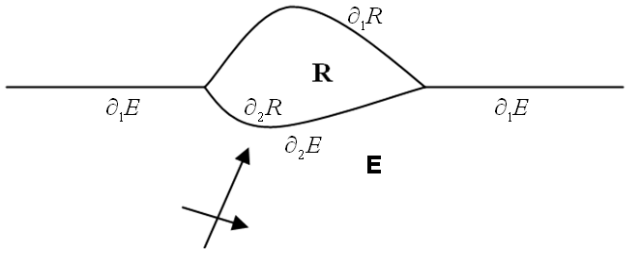

Figure 1. Irregular inclusion R on a half-space E under the incidence of elastic waves.

3.1. Boundary conditions

According to Fig. 1 traction-free boundary condition is reached at the free surface for regions R and E ($\partial_1 R$ and $\partial_1 E$), then this can be represented by writing

$$t_i^R(\boldsymbol{x}) = 0 \qquad \boldsymbol{x} \in \partial_1 R, \tag{3}$$

$$t_i^E(\boldsymbol{x}) = 0 \qquad \boldsymbol{x} \in \partial_1 E. \tag{4}$$

On the other hand, at the common interface between regions *R* and *E*, the continuity of displacements and tractions is given as

$$u_i^R(\boldsymbol{x}) = u_i^E(\boldsymbol{x}) \quad \boldsymbol{x} \in \partial_2 R = \partial_2 E, \tag{5}$$

$$t_i^R(\boldsymbol{x}) = t_i^E(\boldsymbol{x}) \quad \boldsymbol{x} \in \partial_2 R = \partial_2 E. \tag{6}$$

Considering that both tractions and displacements on each region *E* and *R* can be expressed as the contribution of free and diffracted fields, then the eq.(3) to eq.(6) can be written as

$$t_i^R(\boldsymbol{x}) = t_i^{d^R}(\boldsymbol{x}) = 0 \qquad \boldsymbol{x} \in \partial_1 R, \tag{7}$$

$$t_i^E(\boldsymbol{x}) = t_i^{o^E}(\boldsymbol{x}) + t_i^{d^E}(\boldsymbol{x}) = 0 \qquad \boldsymbol{x} \in \partial_1 E, \tag{8}$$

On the other hand, continuity of motion and tractions between regions *R* and *E* is given as

$$u_i^{d^R}(\boldsymbol{x}) = u_i^{d^E}(\boldsymbol{x}) + u_i^{o^E}(\boldsymbol{x}) \qquad \boldsymbol{x} \in \partial_2 R = \partial_2 E, \tag{9}$$

$$t_i^{d^R}(\boldsymbol{x}) = t_i^{d^E}(\boldsymbol{x}) + t_i^{o^E}(\boldsymbol{x}) \qquad \boldsymbol{x} \in \partial_2 R = \partial_2 E, \tag{10}$$

respectively. The super-index 'o' stands for free field, while '*d*' for the diffracted one. Using the integral representations of Eq. (1) for displacements and Eq. (2) for tractions, the equations from Eqs. (7) to (10) can be expressed as:

$$c\phi_i^R(\boldsymbol{x}) + \int_{\partial R} \phi_j^R(\xi) T_{ij}^R(\boldsymbol{x};\boldsymbol{\xi}) dS_\xi = 0, \qquad \boldsymbol{x} \in \partial_1 R, \tag{11}$$

$$c\phi_i^E(\boldsymbol{x}) + \int_{\partial R} \phi_j^E(\boldsymbol{\xi}) T_{ij}^E(\boldsymbol{x};\boldsymbol{\xi}) dS_\xi = -t_i^{o^E}(\boldsymbol{x}), \qquad \boldsymbol{x} \in \partial_1 E, \tag{12}$$

$$\int_{\partial R} \phi_j^R(\boldsymbol{\xi}) G_{ij}^R(\boldsymbol{x};\boldsymbol{\xi}) dS_\xi - \int_{\partial E} \phi_j^E(\boldsymbol{\xi}) G_{ij}^E(\boldsymbol{x};\boldsymbol{\xi}) dS_\xi = u_i^{o^E}(\boldsymbol{x}), \qquad \boldsymbol{x} \in \partial_2 R = \partial_2 E, \tag{13}$$

$$\begin{aligned} c\phi_i^R(\boldsymbol{x}) + \int_{\partial R} \phi_j^R(\boldsymbol{\xi}) T_{ij}^R(\boldsymbol{x};\boldsymbol{\xi}) dS_\xi - c\phi_i^R(\boldsymbol{x}) \\ - \int_{\partial E} \phi_j^E(\boldsymbol{\xi}) T_{ij}^E(\boldsymbol{x};\boldsymbol{\xi}) dS_\xi = t_i^{o^E}(\boldsymbol{x}), \end{aligned} \qquad \boldsymbol{x} \in \partial_2 R = \partial_2 E, \tag{14}$$

respectively.

To solve numerically the system Eqs. (11) to (14), we discretize them using circles to compute the integrals exactly. In general, the boundaries of each region are discretized into boundary elements whose size depends on the shortest wavelength (six boundary segments per wavelength). The force densities ϕ's are taken to be constant along each element and Gaussian

integration (or analytical integration, where the Green's function is singular) is performed. The system to be solved is composed of 3(N+K+2M) equations, where N, M and K are the boundary elements that form the boundaries $\partial_1 E$, $\partial_2 E$ and $\partial_1 R$ ($\partial_2 E = \partial_2 R$). Once the system is solved, the unknown values of the ϕ's are obtained and the diffracted displacement and traction fields are computed by means of Eq.(1) and Eq.(2), respectively. To obtain results in time domain a FFT algorithm is used.

4. The Model

To perform the computations with IBEM we take a simple model. It corresponds to a homogeneous curtain with inclined faces both up and downstream and has two planes of symmetry. The canyon cross-section is triangular. Consider the plane and front views of the triangular canyon and rockfill dam depicted in Fig. 2.

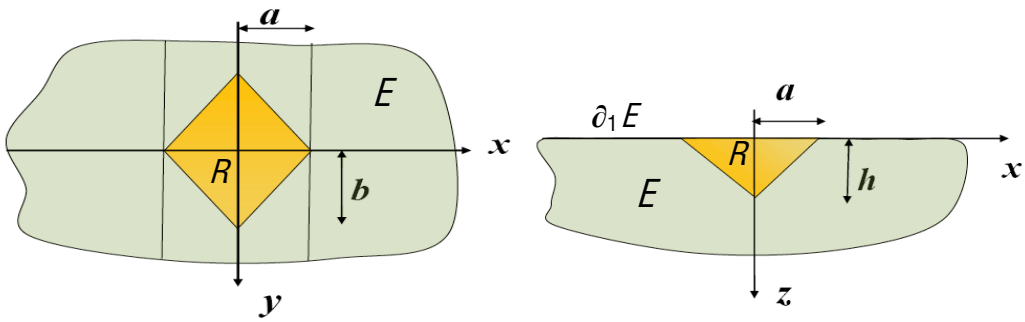

Figure 2. Plane and front views of the triangular canyon and rockfill dam. Here a=b=375 m, h=300 m. The half space has a triangular canyon. The yellow zone corresponds to our homogeneous rockfill.

4.1. Mechanical Properties

The material is assumed elastic, homogeneous, isotropic and with hysteretic damping. The precompression of the materials weights prevents separation of the rock grains. In a linear elastic solid α, β = compressional and shear wave propagation velocities, respectively. They are defined as $\alpha = \sqrt{(\lambda + 2\mu)/\rho}$ and $\beta = \sqrt{\mu/\rho}$ where λ and μ = Lamé elastic parameters and ρ = mass density. Hysteric damping means that in frequency domain wave propagation velocities are made complex by multiplying the nominal value by the factor (1+i/Q) in which $i = \sqrt{-1}$ is the imaginary unit and Q = quality factor (assumed constant). This type of damping helps to approximate linearly inelastic behavior and non linearity. Table 1 shows the said properties for both dam curtain and half-space.

Table 1. Dam and half-space mechanical propertiess

	DAM	HALF-SPACE
α	600 m/s	1200 m/s
β	300 m/s	600 m/s
ρ	1.6 g/cm^3	1.8 g/cm^3
Q	50	100

4.2. Curtain wall structure

Modern rockfill designs substitute the typical impervious core by relatively thin plate of reinforced concrete composed by panels. The stiffness of this component is usually neglected but its integrity implies the revision of strain demand at the model surface.

4.3. Seismic excitation

It is usual to specify at a base of the model a design acceleration time history disregarding the physical meaning of such motions. Such an approach will be revised and discussed elsewhere. Our concern now is to generate a correct seismological background for the modeling of rockfill dams, particularly we are dealing with numerical solution of their response. Our code allows to consider incident P, SV, SH and Rayleigh waves with a given azimuth (relative to ***x*** axis). Incident angles for P, SV and SH waves can vary. Here we consider incidence of P waves with zero and 30 degrees (relative to ***z*** axis) and Rayleigh waves with zero azimuth. Fig. 3 shows 51 receivers equally spaced along the blue line (at $x = 0$). The circles represent the discretization regions that delineate the model geometry. We obtained the surface motion (transfer functions and time series of displacements) at the said receivers.

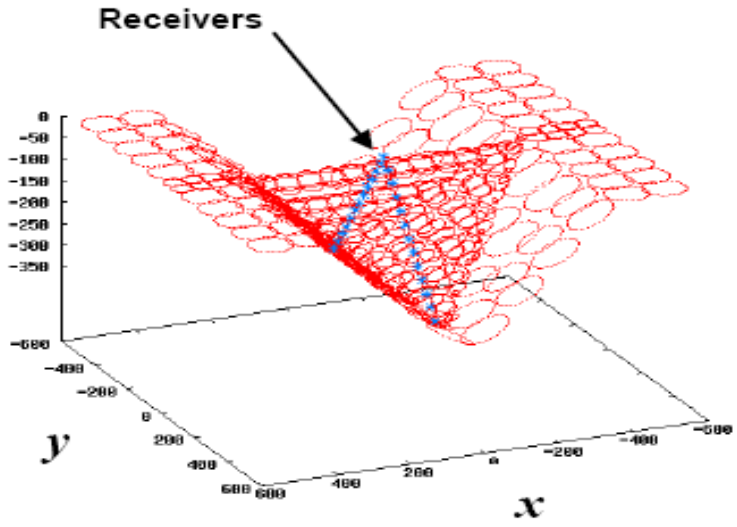

Figure 3. A set of 51 receivers is distributed along the slopes.

5. Results

Using the IBEM we compute the seismic response of a three-dimensional rockfill dam model placed within a canyon that constitutes an irregularity on the surface of an elastic half-space. The rockfill is also assumed elastic with hysteretic damping to account for energy dissipation. Various types of incident waves are assumed to rigorously analyze the physical characteristics of the response: symmetries, amplifications, stress concentrations, impulse response and the like.

5.1. Frequency domain results

This section shows some preliminary results in the frequency domain. Figure 4 shows displacement amplitudes for frequencies 0.8, 1.6, 3.2, and 6.4 Hz. For small frequencies the response are smooth and symmetric. At high frequencies, significant amplifications of vertical motion take place at the middle of the curtain. At the center of profile the horizontal component is null. This shows correct symmetries.

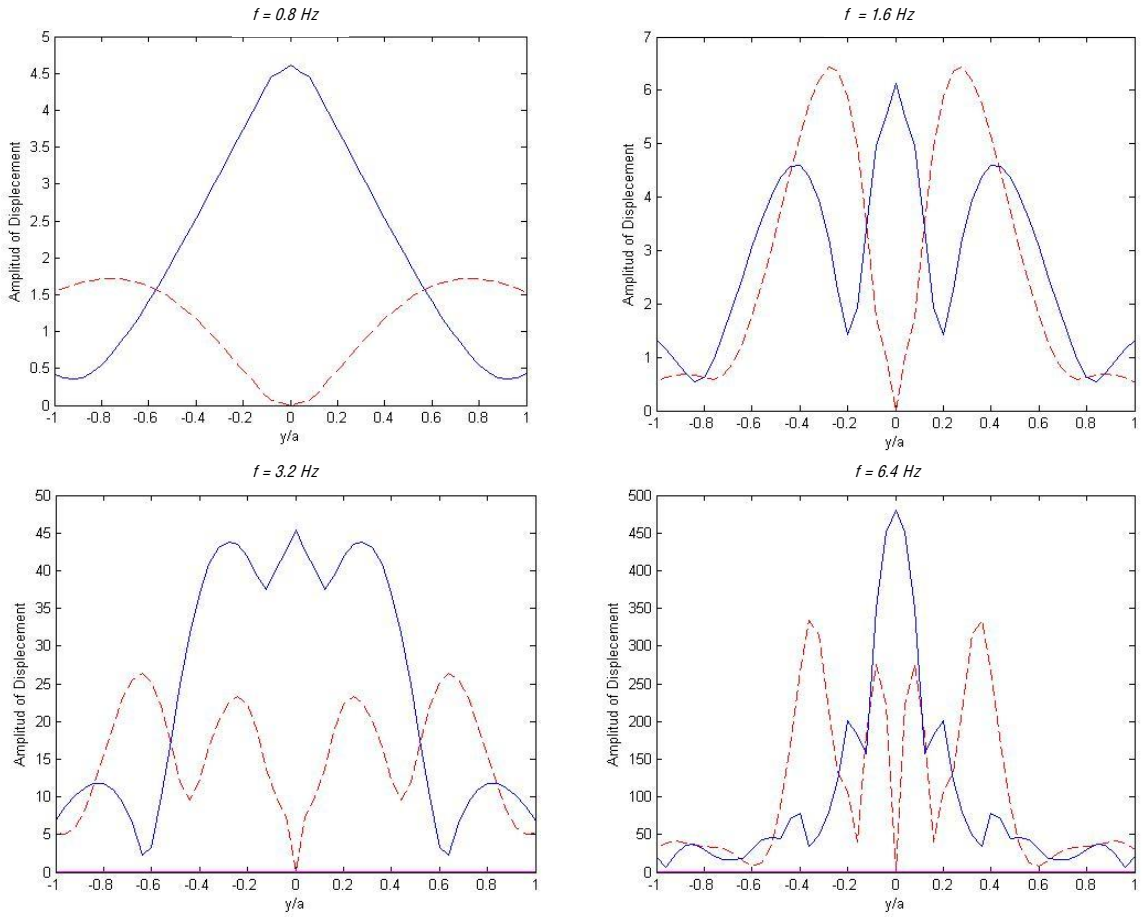

Figure 4. Displacement amplitude for 51 equally spaced receivers located on the curtain along the dam slopes (x=0). Normal incidence of P wave. Dotted red line shows displacement for the v component and the solid blue line corresponds to the vertical component w.

5.2. Synthetic Seismograms

Figure 5 depicts synthetic seismograms. Incident Rayleigh waves take most of the energy for $w(0, y)$ and we can see a short arrival due to amplifications caused by the topography along the curtain. The wedge like geometry of the curtain has an influence on the displacements of the vertical component $w(0, y)$ under a P wave incidence. Due to the symmetry of the curtain, when we place a line of receivers along it, we can seen some symmetries and it is even possible to find an analytic solution for this simple 2-D case.

Seismograms in Figure 6 show that incident P waves produce more diffraction just at the middle of the line where the receivers are placed (i.e. exactly where the crown is located). This diffraction might be due to the superposition of internal multiple reflections of waves generated at the edge of the crown and the semi-space. These waves are vertically reflected towards the crown, where the arrival time for incident waves is less and the displacements are symmetric.

6. Discussion

A full 3D analysis of heterogeneous medium can be extremely expensive and not fully justified because it is difficult to count with a complete description of the heterogeneous material. The BEM and the IBEM offer the possibility to account for topographical effects economically and simply.

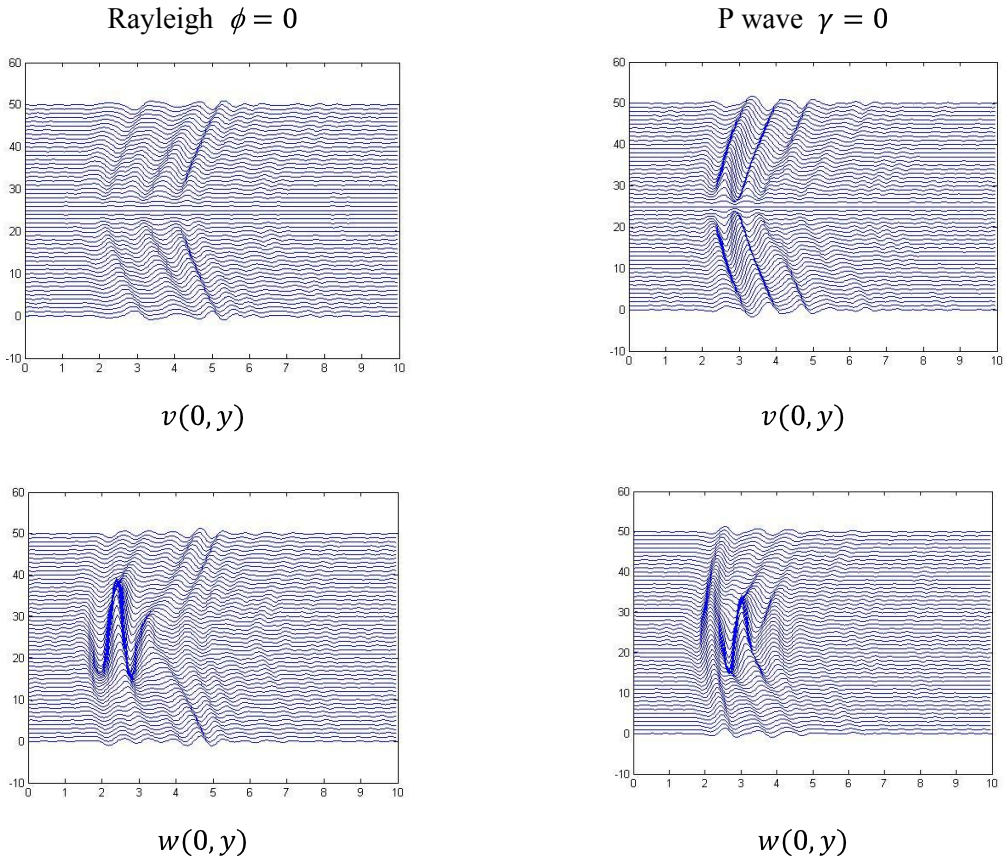

Figure 5. Synthetic seismograms for *v* and *w* at 51 receivers equally spaced along the y axis. Dam under incidence of Rayleigh waves (left) and P waves at $\gamma = 60$ degrees (right). The incident waveform is a Ricker wavelet with characteristic period of $t_p = 0.5$ sec.

Our preliminary results using the IBEM are consistent. Computations are performed in the frequency domain and lead to time response using Fourier analysis. Tests and validations with BEM implementations, including one that uses the FMM (Fast Multipole Method) [11, 12] are under way.

7. Conclusions

Usually, the seismic response of rockfill dams is simulated using either finite elements (FEM) or finite differences (FDM). In most applications, commercial tools that combine features of these methods are used to assess the seismic response of the system for a given motion at the base of model. However, in order to consider realistic excitation of seismic waves with different incidence angles and azimuth we explore the IBEM.

We applied the IBEM to solve the integral representation of eq.(1) only for boundary elements in the domain. It is possible to compute stresses and tractions by directly applying Hooke's law. This is one of the advantages of IBEM. Furthermore, the system of linear equations is smaller than the resulting when using other methods such as FEM of FDM. Domain methods work with big meshes when dealing with infinite spaces (i.e. half-space or full space), whereas IBEM can naturally treat infinite space only discretizing the boundary of interest. Further work is needed to implement this method for more complex geometries and to consider solid-fluid interactions.

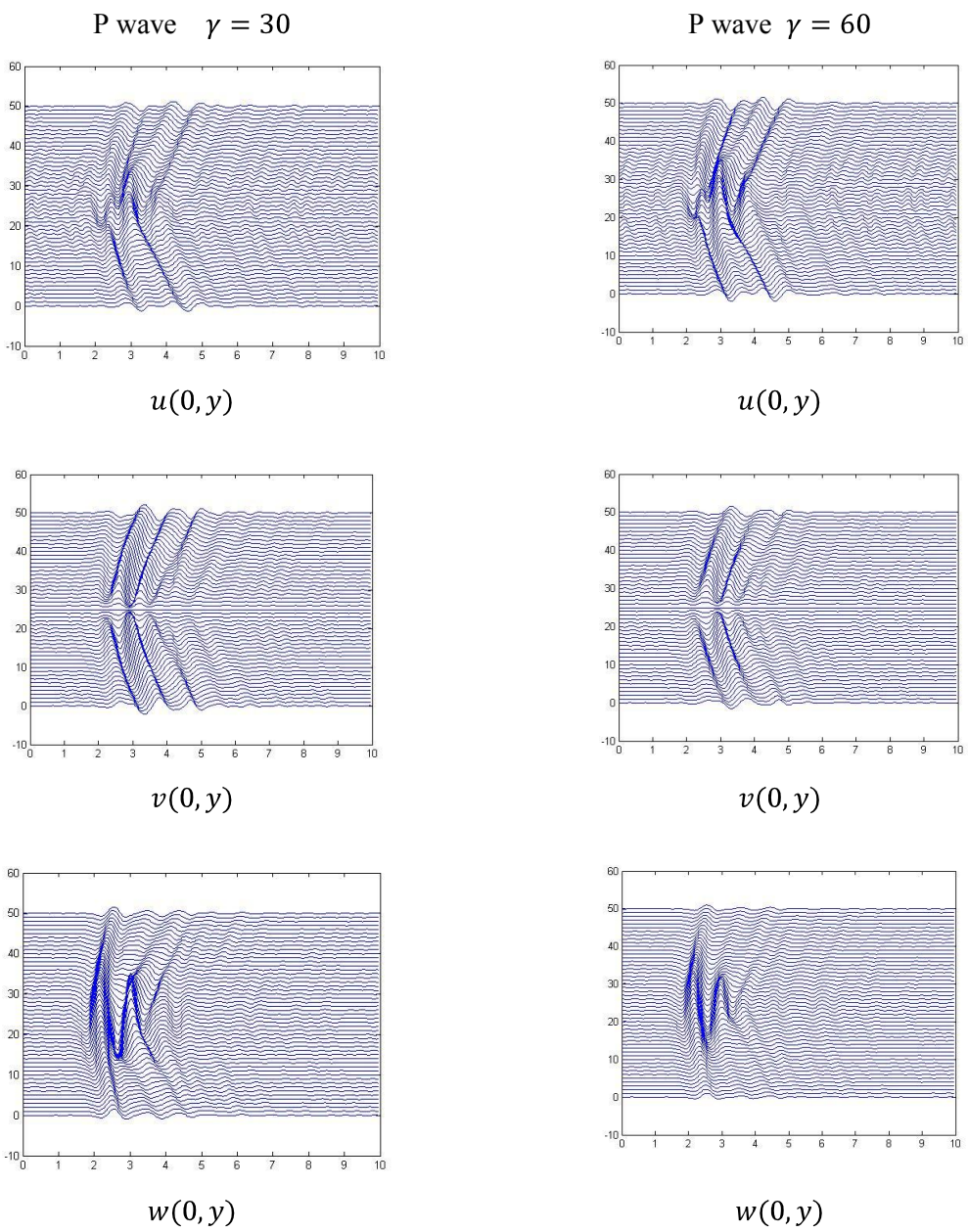

Figure 6. Synthetic seismograms for u,v and w at 51 receivers equally spaced along the *y* axis. The range of y is between -*a* to *a*, where *a*=375 m. Dam under incidence of P waves at *γ=30* degrees (left) and γ =*60* degrees (right).The incident waveform is the same as the Figure 3.

8. Acknowledgements

The partial supports from Comisión Federal de Electricidad, Mexico, and DGAPA-UNAM under Grant IN121709 are greatly appreciated.

9. References

[1] Dakoulas P and C-H- Hsu (1995), "Response of Dams in Semielliptical Canyons to Oblique SH waves", *Journal of Engineering Mechanics ASCE* 121, 379-391.

[2] Papalou A and J Bielak (2001), "Seismic Elastic Response of Earth Damps with Canyon Interaction", *Journal of Geotechnical and Geoenvironmental Engineering ASCE* 127, 446-453.

[3] Maeso O, J J Aznárez and J Domínguez (2002). "Effects of Space Distribution of Excitation on Seismic Response of Arch Dams", *Journal of Engineering Mechanics*, 128: 759–768.
[4] Maeso O, J J Aznárez and J Domínguez (2004). "Three-dimensional models of reservoir sediment and effects on the seismic response of arch dams", *Earthquake Engineering and Structural Dynamics* 33:1103–1123.
[5] Aki K (1988), "Local site effects on strong ground motion", *Earthq. Eng. And Soil Dyn. II: Recent Advancesin Ground Motion Evaluation*, J. L. Von Thun (Editor), Geotechnical Special Publication No.20, Am. Soc. Civil Eng., New York, 103-55.
[6] Geli, L, P-Y Bard y B Jullien (1988), "The effect of topography and earthquake ground motion: a review and new results" , *Bull. Seism. Soc. Am.* 78, 42-63.
[7] Sánchez-Sesma, F J (1987), "Site effects on strong ground motion", *Intl. J. Soil Dyn. Earthq. Eng.* 6, 124-132.
[8] Sánchez-Sesma, F J and M Campillo (1991). Diffraction of P, SV and Rayleigh waves by topographic features: a boundary integral formulation, *Bull Seism Soc Am* 81, 2234-2253.
[9] Sánchez-Sesma F J y Luzón F (1995), "Seismic response of three-dimensional alluvial valleys for incident P, S and Rayleigh waves", *Bull. Seism. Soc. Am.* 85, 269-284.
[10] Kupradze,V.D (1963).Dynamical Problems in Elasticity, in *Progress in Solid Mechanics*,vol. 3,I.N. Sneddon and R. Hill (Editors). North Holland Amsterdam.
[11] Fujiwara H (2000)."The fast multipole method for solving integral equations of three-dimensional topography and basin problems". *Geophys. J. Int.*, 140:198-210.
[12] Chaillat S, M Bonnet, J F Semblat (2009). "A new fast multi-domain BEM to model seismic wave propagation and amplification in 3D geological structures", *Geoph. J. Int.* 177, 509-531.